JOURNAL OF SPACECRAFT AND ROCKETS
Vol. 39, No. 5, September–October 2002

Multidisciplinary Analysis of a Lifting Body Launch Vehicle

Paul V. Tartabini,* Kathryn E. Wurster,† J. J. Korte,‡ and Roger A. Lepsch§
NASA Langley Research Center, Hampton, Virginia 23681

As part of phase 2 of the X-33 Program, NASA selected an integrated lifting body/aerospike engine configuration as the study vehicle for the conceptual analysis of a single-stage-to-orbit reusable launch vehicle. A team at NASA Langley Research Center participated in the screening and evaluation of a number of proposed vehicle configurations in the early phases of the conceptual design process. The performance analyses that supported these studies were conducted to assess the effect of the vehicle's lifting capability, linear aerospike engine, and metallic thermal protection system on the weight and performance of the vehicle. These performance studies were conducted in a multidisciplinary fashion that indirectly linked the trajectory optimization with weight estimation and aerothermal analysis tools. This approach was necessary to develop optimized ascent and entry trajectories that met all vehicle design constraints. Significant improvements in ascent performance were achieved when the vehicle flew a lifting trajectory and varied the engine mixture ratio during flight. Also, a considerable reduction in empty weight was possible by adjusting the total oxidizer-to-fuel and liftoff thrust-to-weight ratios. However, the optimal ascent flight profile had to be altered to ensure that the vehicle could be trimmed in pitch using only the flow diverting capability of the aerospike engine. Likewise, the optimal entry trajectory had to be tailored to meet thermal protection system heating rate and transition constraints while satisfying a crossrange requirement.

Nomenclature

C_L	=	lift coefficient
I_{sp}	=	specific impulse, s
M_e	=	edge Mach number
M_∞	=	freestream Mach number
O/F	=	total oxidizer-to-fuel ratio
q	=	dynamic pressure, psf
$q \cdot \alpha$	=	dynamic pressure times angle-of-attack, psf · deg
Re_θ	=	momentum thickness Reynolds number
S	=	aerodynamic reference area, ft^2
T/W	=	thrust-to-weight ratio
$(T/W)_{eng}$	=	engine thrust-to-weight ratio
W	=	entry weight, lb
W_{empty}	=	empty weight, lb
W_{ins}	=	inserted weight, lb
X/L	=	body position over vehicle length
α	=	angle of attack, deg
Δ payload	=	change in payload from

Introduction

MANY papers have been written describing the difficulty of designing a fully reusable single-stage-to-orbit (SSTO) launch vehicle.[1–3] The physical difficulty of this problem is exacerbated by the large degree of coupling between the various design disciplines. Nearly every subsystem design decision has far reaching consequences that must be evaluated in a multidisciplinary fashion to assess the impact on the weight and performance of the entire vehicle. This paper discusses this process as it relates to the conceptual design and analysis of an integrated lifting body/aerospike engine reusable launch vehicle (RLV) concept.

From 1996 to 2001, the X-33 technology development program was run as a joint venture between NASA and Lockheed Martin Skunk Works (LMSW). Part of the program included the conceptual design and analysis of a full-scale SSTO vehicle. The primary study vehicle used in these analyses was LMSW's VentureStar™ RLV, which included a number of unique features that differentiated it from other SSTO concepts evaluated in the past.[4] Chief among these differences was the integration of an aerospike engine with a lifting body design. The linear aerospike engine integrated well with the lifting body shape, which helped reduce the weight and complexity of the thrust structure. In addition, the aerospike had performance that was comparable to state-of-the-artbell nozzles but operated at lower stagnation pressures, providing potential weight and operational advantages, and it could be differentially throttled for pitch control, eliminating the need for gimbal actuators. Moreover, a lifting body offered potential weight savings through the reduction of lifting surfaces, and its increased planform area helped reduce entry temperatures, thus enabling more extensive use of a metallic thermal protection system (TPS), which may be more operationally cost-effective than alternative high-temperature ceramic tiles. The VentureStar configuration is shown in Fig. 1.

The analyses and methodologies presented in this paper were developed as the result of a cooperative effort between the NASA Langley Research Center (LaRC) and the Lockheed vehicle developers to mature the conceptual analysis of the full-scale RLV. During this phase of concept maturation, LaRC participated in the design, analysis, and screening of different vehicle concepts and configurations.[5] Throughout the duration of the LaRC study, the feasibility of numerous configurations was evaluated in terms of vehicle mass and payload capability. These mass properties are directly related to the overall performance of the vehicle. Because many design parameters affect both weight and performance, accurate determination of vehicle sizing information requires a multidisciplinary approach to performance analysis. The approach utilized in this study indirectly coupled trajectory optimization, weight estimation, and heating analysis tools to ascertain the impact of various design options on the payload capability of each configuration. With this approach, trade studies were conducted to maximize vehicle performance and cost effectiveness. The primary objective of these studies was to address design issues that presented opportunities and challenges that were unique to the integrated lifting body/aerospike

Presented as Paper 2000-1045 at the 38th Aerospace Sciences Meeting, Reno, NV, 10–13 January 2000; received 11 March 2000; revision received 2 March 2002; accepted for publication 26 March 2002.

*Research Engineer, Vehicle Analysis Branch, Mail Stop 365. Member AIAA.
†Senior Research Engineer, Vehicle Analysis Branch, Mail Stop 365. Associate Fellow AIAA.
‡Senior Research Engineer, Multidisciplinary Optimization Branch, Mail Stop 159. Senior Member AIAA.
§Senior Research Engineer, Vehicle Analysis Branch, Mail Stop 365. Member AIAA.

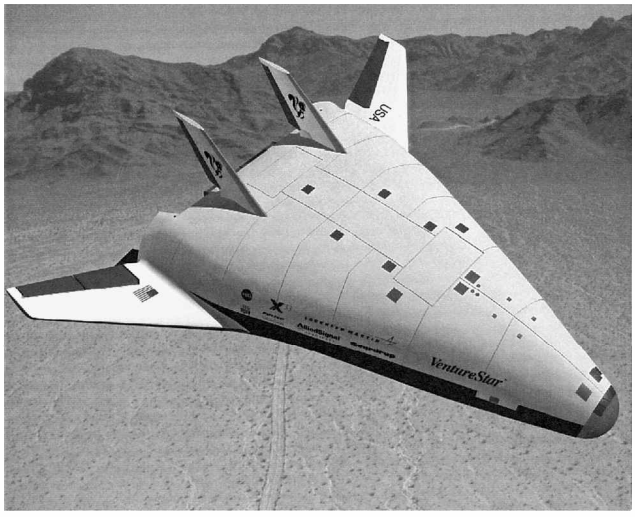

Fig. 1 VentureStar configuration.

vehicle concept. Specifically, this paper addresses issues that pertain to 1) the effect of the vehicle's lifting capability and aerospike engine on ascent performance, 2) the ability to influence vehicle sizing by varying the engine size and mixture ratio, and 3) the ramifications of the metallic TPS on the entry trajectory design. A multidisciplinary approach was the only way to ensure that the system fully exploited the performance benefits offered by the vehicle design while staying within the operational limits imposed by its cost-saving elements.

Approach

Many of the trades discussed in this paper required the calculation of various physical characteristics of the vehicle, including payload capability, empty weight, and gross lift-off weight (GLOW). These quantities were predicted using a multidisciplinary analysis that included trajectory optimization, weights and sizing estimation, and engine performance prediction.

Trajectory optimization, which formed the core of this analysis method, was performed using the three-degree-of-freedom version of POST.[6] This program has been developed as a joint government/contractor effort, and it is available and widely used within the aerospace community. Inputs to this code include Earth atmospheric and gravitational models, system mass properties, engine performance, and vehicle aerodynamics.

Mass property estimation was conducted using CONSIZ.[7] CONSIZ utilizes parametric mass-estimating relationships based on historical regression, finite element analysis, and technology readiness level. With knowledge of the vehicle layout, CONSIZ can also be used to estimate the location of the vehicle c.g. for trim calculations. In this paper, mass property data were generated by LaRC using CONSIZ and were calibrated to weight statements released by LMSW. Another required input to POST was a propulsion data model that was computed using a suite of computer codes that simulated linear aerospike engine performance. These codes were able to generate an aerospike engine database as a function of altitude, mixture ratio, power level, and thrust vectoring for use within the POST trajectory code. The capabilities and development of these tools, as well as representative aerospike performance data, are presented in Ref. 8. A final input to the trajectory optimization was an aerodynamic database that included coefficients for lift, drag, and pitching moment as a function of Mach number, angle of attack, and control surface deflection. This database was obtained through the blending of solutions from computational methods and wind-tunnel data. Updates to the aerodynamic coefficients were made periodically during the conceptual design phase to reflect configuration shape changes.

All of the entry performance trades discussed in this paper were performed using POST and MINIVER.[9] POST was the ideal tool to perform entry trajectory optimization, but was limited in its ability to provide heating environments. An aerothermal analysis tool, MINIVER, was chosen to complement POST and to provide a reliable measure of the heating levels during trajectory development. MINIVER is an engineering code that uses approximate heating methods with simple flowfield and geometric shapes to model heating on critical regions of the vehicle. MINIVER has been used extensively as a preliminary design tool and has demonstrated excellent agreement with more detailed heating solutions for stagnation and windward acreage areas on a wide variety of vehicle configurations.[10–12] In addition to providing sufficiently accurate heating levels, it can be used to estimate the onset of transition to turbulent flow.

Results and Discussion

Ascent Performance

The reference mission used for this analysis was delivery of a 25,000-lb design payload to the International Space Station (ISS). The reference ascent trajectory began with launch at NASA Kennedy Space Center and ended with the insertion of the payload into a 50×248 n mile orbit inclined 51.6 deg. At this point, the RLV coasted to apogee, where the orbital maneuvering system engines were used to circularize at the ISS altitude. The figure of merit used for the ascent trade studies was payload capability. This parameter was determined for each vehicle assuming a constant propellant volume, which ensured that the vehicles being compared were similar in size (dry weight), thus minimizing errors due to scaling. That is, the vehicle size was fixed for these trades with the payload targeted at 25,000 lb but allowed to vary according to changes in ascent performance.

The aerospike engine performance reflected the propulsion system at the conclusion of this study with eight engines operating at a chamber pressure of 2500 psia and an area ratio of 196. Reference 8 discusses a version of this database that was created to provide realistic engine performance across the mixture ratio/power level envelope, thereby minimizing the amount of interpolation error.

The reference ascent trajectory was determined by maximizing the weight inserted into the target orbit. The point of insertion into the target orbit was free. The trajectory was optimized by adjusting the pitch attitude, engine power level, and engine mixture ratio flight profiles. These control variables were constrained by angle of attack and engine operating limits. An additional constraint was imposed on the mixture ratio profile, which had to be varied such that the ratio of oxidizer to fuel was consistent with the vehicle tank design value of 6.0. The optimized trajectory had to meet a number of inflight constraints, including limits on axial acceleration, dynamic pressure, $q \cdot \alpha$, and angle of attack. The parameter $q \cdot \alpha$ is proportional to the structural loading of the vehicle during flight and is the product of dynamic pressure and angle of attack. Also, the reference trajectory was untrimmed. A trimmed case required an engine database that modeled the thrust vector control capability of the aerospike. This part of the database became available in the later stages of the program as the fidelity of the engine models increased. A subsequent section will discuss the effect of a trim constraint on vehicle performance. The values of all flight constraints and control limits are listed in Table 1.

The significant flight parameter profiles for the reference ascent trajectory are shown in Figs. 2a and 2b. Main engine cutoff (MECO) took place near perigee of the transfer orbit, at an altitude of 57 n mile and a flight path angle near 0.1 deg. The peak dynamic pressure of 540 psf occurred at a Mach number of 1.1 and the $q \cdot \alpha$ limit of 1500 psf · deg was held for roughly 25 s, from Mach 0.4 to 0.6.

Table 1 Constraints imposed on nominal ascent trajectory.

Constraint name	Constraint value
Final orbit	50×248 n mile
Final inclination	51.6 deg
Axial acceleration limit	$a_x \leq 3\ g$
Dynamic pressure limit	$q \leq 600$ psf
$q \cdot \alpha$ limits	$\lvert q \cdot \alpha \rvert \leq 1500$ psf
Angle-of-attack limits	$-4 \leq \alpha \leq 12$ deg
Liftoff thrust to weight ratio	1.35
Overall tank ratio	6.0
Engine power level	$0.2 \leq$ power level ≤ 1.0
Engine mixture ratio	$5.5 \leq$ mixture ratio ≤ 7.0

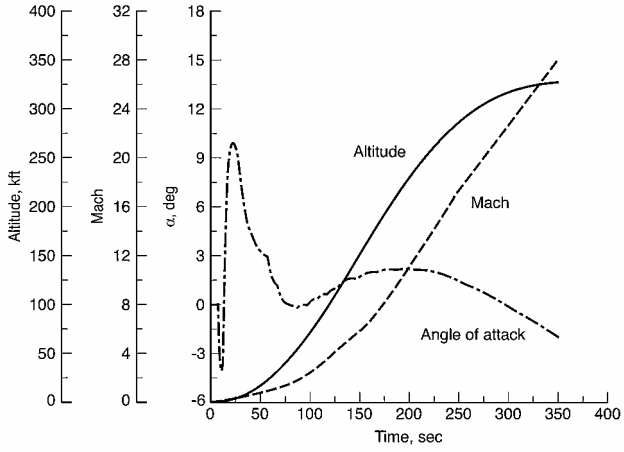

a) Altitude, Mach, and angle-of-attack profiles

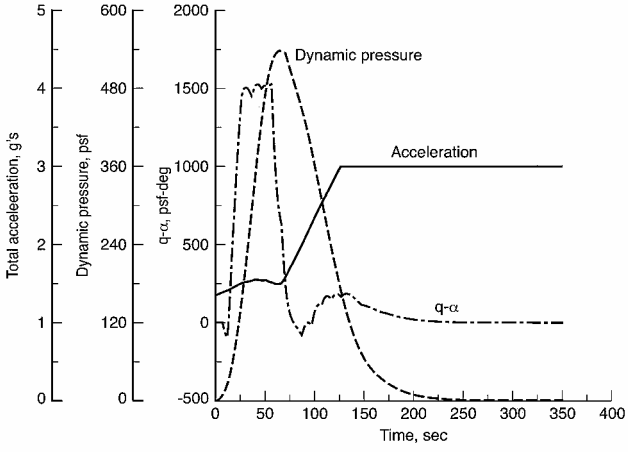

b) Acceleration, dynamic pressure, and $q \cdot \alpha$ profiles

Fig. 2 Important flight parameter profiles for the nominal ascent trajectory.

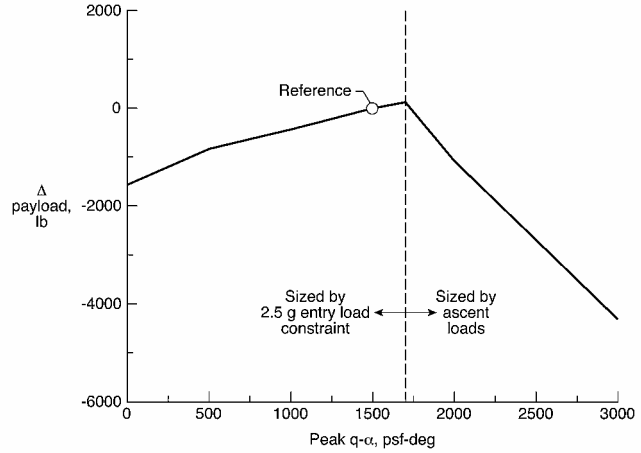

Fig. 3 Effect of the $q \cdot a$ structural design constraint on vehicle payload capability.

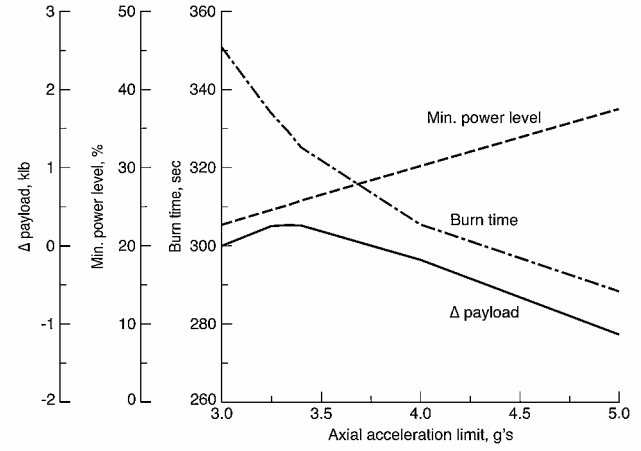

Fig. 4 Effect of the axial acceleration limit on vehicle payload capability.

When these two structural constraints are maintained throughout the trajectory, the peak normal force was limited to 2.3 times the landed weight of the vehicle, which was less than the allowable normal load factor of 2.5 expected to be reached during entry. The engine was flown at 100% power level from liftoff until the 3-g axial acceleration limit was reached at approximately 125 s into flight ($h = 112{,}000$ ft, $M = 4.2$). At this point, the engine was gradually throttled down to nearly 20% at MECO to maintain the 3-g limit. The engine mixture ratio was varied continuously throughout ascent. The manner in which this parameter is varied during flight has a significant effect and will be discussed in more detail later.

Structural Constraint

The reference ascent trajectory was designed to take advantage of the lifting ability of the vehicle. When a lifting trajectory was flown, it was possible to decrease the amount of gravity losses significantly, thereby improving vehicle performance and payload capability. However, increasing the amount of lift during ascent generally required flight at higher angles of attack and resulted in greater stress on the vehicle structure. Accordingly, the reference ascent trajectory was constrained to limit the parameter $q \cdot \alpha$ to 1500 psf · deg to ensure that the peak normal force did not exceed 2.5 times the landed weight, which was the structural load that the vehicle was designed to withstand during entry and landing.

The effect of the $q \cdot \alpha$ constraint on vehicle performance is shown in Fig. 3. There was a considerable benefit associated with using lift during ascent because flying a nonlifting trajectory resulted in a payload penalty of over 1500 lb when compared to the reference case. As long as the maximum load factor was kept below the 2.5 entry design limit, the payload capability increased as the $q \cdot \alpha$ limit was raised because the vehicle could use more lift to further reduce gravity losses. However, once the design limit was exceeded, additional structure was needed to sustain the larger loads. The weight penalty associated with this added structure was estimated by increasing the size of the wing to account for the higher aerodynamic loading. There was no benefit to increasing the $q \cdot \alpha$ limit beyond 1700 psf · deg (where the peak normal load factor was 2.5) because the wing weight penalty was severe enough to cause an overall degradation in payload capability. Even though trajectories that achieved these higher values of $q \cdot \alpha$ had the benefit of more lift, the actual increase in ascent performance was minimal because increased drag losses, which are also incurred when flying a lifting trajectory, began to offset the reduction in gravity losses. Consequently, when ascent loads were used to size the vehicle, the growth in the weight of the wings dominated any small increases in performance, and the net effect was a reduction in vehicle payload capability.

Axial Acceleration Limit

A series of ascent trajectories was optimized at a range of axial acceleration constraints from 3 to 5 g. Changing this constraint had a small effect on the vehicle payload capability (Fig. 4). Increasing the acceleration limit from 3.0 to 3.3 g resulted in slightly lower gravity losses, which led to an additional 300 lb of payload capability. As the limit was increased beyond 3.3 g, the lower gravity losses were eradicated by an increase in thrust vectoring losses (the ΔV required to turn the velocity vector). To insert into a 50 × 248 n mile orbit, the vehicle had to perform much of its pitchover at altitudes high enough to avoid accumulating excessive drag losses. As the g limit was increased, the velocity at which this pitchover occurred became higher, and more energy had to be expended to turn the velocity vector. Although changing the acceleration limit had a small effect on payload capability, increasing the limit may be beneficial to the engine development because a higher limit enables higher power

levels at MECO and shorter burn times (Fig. 4). The former could facilitate the design of the engine control system, whereas the latter may increase the overall engine life.

Pitch Trim Capability

The vehicle was required to be trimmed during ascent using only thrust vector control (TVC) supplied by the linear aerospike engine. The aerospike could produce a thrust moment to counteract the aerodynamic pitching moment of the vehicle by diverting up to 15% of the outflow from the top engine banks to the bottom engine banks, or vice versa. Diverting the flow created a couple from the difference in axial force between the top and bottom of the engine (although the net axial force remained unchanged). This couple was the largest contributor to the total thrust moment. (There was an additional smaller contributor due to differences in the normal force acting on the top and bottom engine ramps.) An engine performance database created by LaRC that included TVC data was used to assess the impact of a trim constraint on the reference ascent trajectory. The trimmed trajectory was designed such that no more than 50% of the control authority was used throughout the ascent. The vehicle c.g. was varied linearly with weight from the liftoff position of 39.9% of the reference length (nose to cowl) to the MECO value of 77.6%. To keep the amount of TVC used below 50%, the angle of attack had to be kept within the envelope shown in Fig. 5. Note that the TVC effectiveness varied with altitude and was lowest at 35 kft, where the angle of attack had to be kept within a 1.3-deg window. Also in Fig. 5, the angle-of-attack profile for the trimmed ascent trajectory is compared to the untrimmed reference trajectory. At altitudes below 40,000 ft, the angle of attack had to be kept lower than optimal to meet the trim constraint. When the angle of attack was limited, less lift was available for reducing gravity losses, and the result was an 1100-lb penalty in vehicle payload capability.

The reference configuration discussed in this paper had the liquid oxygen (LOX) tank positioned in the nose. One trade that was considered by the LaRC team was moving the LOX tank to the aft end of the vehicle, which could potentially decrease the weight of the liquid hydrogen (LH_2) tank and the intertank structure significantly. One concern with moving the LOX tank aft, however, was the effect of the resulting rearward shift in c.g. location on the ability of the vehicle to trim during ascent. The effect of pitch trim was computed for two LOX aft vehicles that were modeled as having a constant c.g. position during ascent at locations of 78 and 82% of the reference body length (nose to cowl), respectively. Figure 6 compares the trim capability of these LOX aft configurations with the reference LOX forward configuration. These results show that the TVC requirements actually decreased the more the longitudinal c.g. was moved aft. This behavior occurred because most of the thrust moment was due to the couple created by the difference in axial force between the top and bottom engine banks. Because this couple was independent of longitudinal c.g. position, the maximum attainable thrust moment did not change much as the c.g. was moved. The effect of the c.g. location was much stronger on the aerodynamic

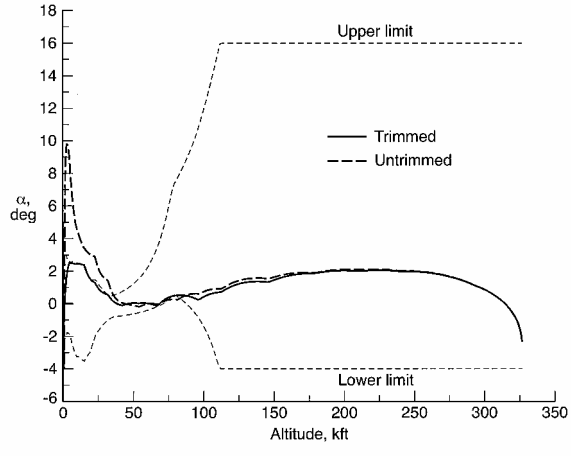

Fig. 5 Effect of trim constraint on angle-of-attack profile for nominal ascent trajectory.

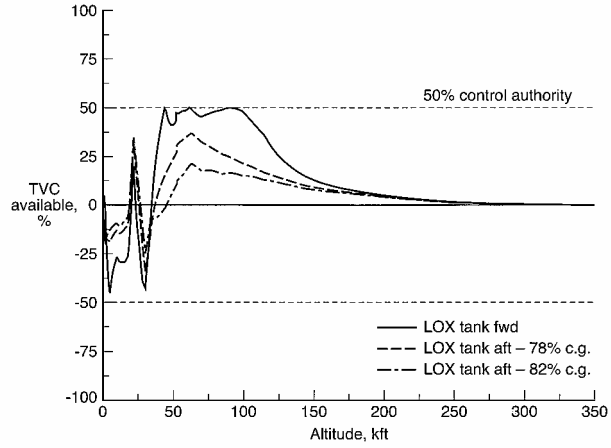

Fig. 6 Comparison of required TVC profiles for the reference vehicle and two LOX-aft configurations.

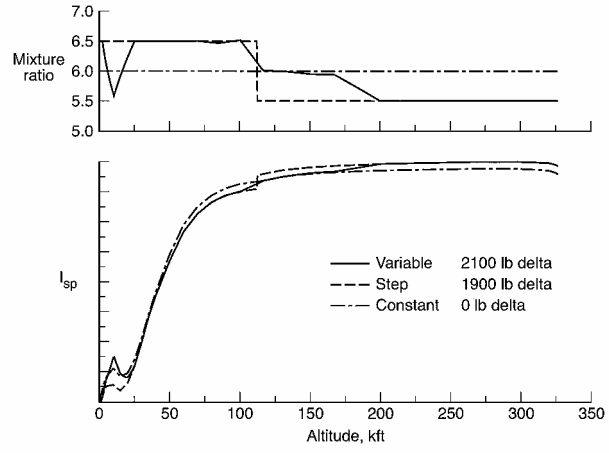

Fig. 7 Engine mixture ratio profiles and corresponding effect on I_{sp} trend during flight.

moment, and a rearward shift in c.g. generally resulted in smaller aerodynamic moments for the low angles of attack seen during ascent. Therefore, the net effect of moving the LOX tank aft was to increase the pitch trim control margin. With an increase in the control margin, higher angles of attack can be flown in the flight regime where the trim constraint is most critical, enabling a more optimal ascent trajectory to be flown. Although moving the LOX tank aft may ease pitch trim concerns during ascent, more work is necessary to understand the effect of such a move on pitch trim during entry.

Engine Performance Trades

With the aerospike engine it was possible to vary the mixture ratio between values of 5.5 and 7.0 during flight. In general, as the engine mixture ratio was increased, total thrust increased and the specific impulse I_{sp} decreased. Ideally the mixture ratio should be set high early in flight, where high thrust levels are required to accelerate the fuel-heavy vehicle, and later transitioned to the lowest allowable value to maximize vacuum I_{sp}. Generally, engine development becomes more complicated and expensive as the flexibility of the engine to vary mixture ratio is increased.

A performance assessment was made for three different modes of mixture ratio adjustment during flight (constant, step, and continuously varying). In cases where the mixture ratio was varied, the total O/F ratio (the ratio of total LOX weight to total LH_2 weight) had to be kept consistent with the vehicle propellant tank design. (Reference O/F was 6.0.) The mixture ratio profiles for each case are shown in Fig. 7 along with the corresponding effect that each had on the I_{sp} trend. By continuous variation of the mixture ratio, the inserted weight could be increased by 1900 lb over the constant case and 200 lb over the step case. In the step and variable cases, the mixture ratio was initially set to 6.5 because the slight increase

in thrust that could be gained by increasing the mixture ratio to 7.0 was overpowered by a greater loss in I_{sp}. The variable case differed from the step case at low altitudes because the mixture ratio profile could be tailored to take advantage of a lower I_{sp} caused by shock interference with the nozzle wall.[8] The profile differed at higher altitudes because it was more efficient to lower the thrust to meet the g limit by decreasing mixture ratio (variable case) rather than power level (step case). The added design complexity of a continuously varying engine over one that performs a step change may not be worth the small accompanying performance increase.

Vehicle Sizing Studies

The liftoff T/W and total O/F ratios were critical parameters that influenced the weight and performance of the vehicle. Because both of these parameters affected weight and performance in opposite ways, it was important to link the weight estimation and trajectory optimization to capture the combined effect. An iterative process was undertaken that coupled the results of POST and CONSIZ. This process began with an initial guess of the mass ratio (GLOW/W_{ins}), which is a measure of vehicle performance. Next, values for the liftoff T/W and O/F ratio were selected. All three of these parameters were input into CONSIZ to determine their effect on the empty weight of the vehicle. The mass ratio essentially determined the total propellant load of the vehicle. The liftoff T/W was directly proportional to the size of the engine and impacted the weight of the propulsion system (engines, feed system, etc.) and thrust structure. The total O/F ratio determined the propellant bulk density and, consequently, affected the weight of the tanks and propellants.

In this analysis, CONSIZ was used to size the vehicle to deliver a 25,000 lb payload to the ISS. That is, as changes were made to mass ratio, liftoff T/W, and the total O/F, the vehicle was photographically scaled to maintain a fixed 25,000-lb payload. Favorable changes to these three parameters resulted in a vehicle that was smaller than the reference configuration (in physical dimensions and empty weight) and could still deliver the required payload. The vehicle was scaled under the assumption that the volumetric efficiency (ratio of tank volume to total volume) remained constant. The impact of this assumption was not significant because vehicles were not scaled by huge amounts (less than 15% throughout the study) and the results were concerned primarily with changes in empty weight rather than absolute values. With this technique, the effect of the liftoff T/W and total O/F on the empty weight was determined with the assumption that a vehicle with a lower empty weight would ultimately have lower development costs.

The other key component of this iterative sizing process was the optimization of the ascent trajectory using the weights calculated with CONSIZ. The same mission and constraints listed in Table 1 were used in the trajectory calculations. For each optimized trajectory, the engine performance model was scaled to meet the required liftoff T/W, and the engine mixture ratio was varied such that the total O/F was consistent with what was used in the weight calculation. Trajectories were determined that maximized the weight inserted into orbit (which was equivalent to the lowest possible mass ratio). Once the minimum mass ratio was determined from the trajectory optimization, it was fed back into CONSIZ, and this whole process was repeated until convergence. This entire multidisciplinary analysis was performed for enough values of T/W and O/F to demonstrate how the empty weight changed with respect to the reference vehicle.

The effect of the total O/F ratio on the empty weight is shown in Fig. 8. All values have been normalized with respect to the reference vehicle ($T/W = 1.35$ and $O/F = 6.0$). Changing the O/F ratio had a notable effect on empty weight and led to differences of more than 5% between the best and worst values. The optimal O/F value for a liftoff T/W of 1.35 was approximately 6.5 and was characterized by a reduction in empty weight of over 2.5% from the reference. Two additional curves are shown in Fig. 8 to demonstrate the importance of coupling the performance and sizing analyses. When only performance changes due to varying the total O/F were considered (i.e., weight changes due to varying the propellant bulk density were neglected), the empty weight increased rapidly as the total O/F was

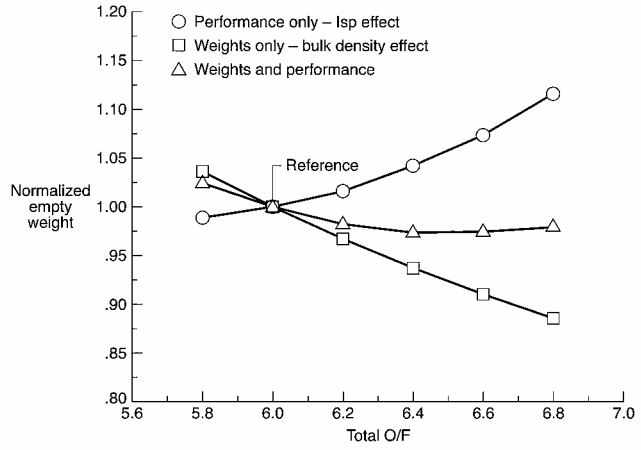

Fig. 8 Variation of vehicle empty weight with total *O/F* ratio (normalized with reference).

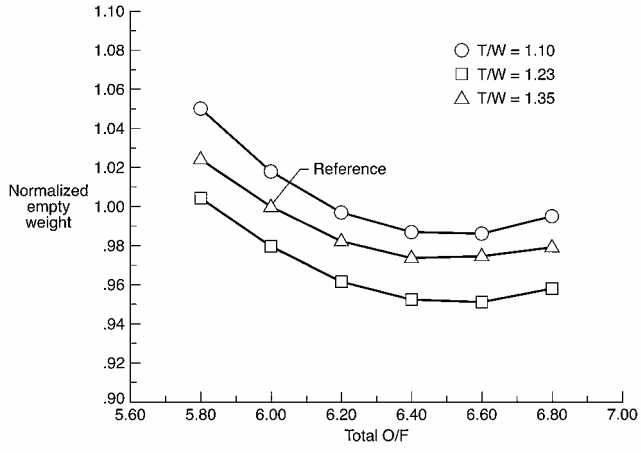

Fig. 9 Effect of liftoff *T/W* on optimal *O/F* ratio (normalized with reference).

raised. This increase occurred because the engine had to operate at high mixture ratios for a longer duration during the trajectory to raise the total O/F, thus decreasing the average I_{sp} and increasing the mass ratio. On the other hand, if the mass ratio was assumed to remain constant as the total O/F ratio was changed (i.e., the effect of total O/F on performance was neglected) then the empty weight went down as the total O/F was increased. This improvement in empty weight occurred because of the increase in propellant bulk density resulting from the higher ratio of LOX to LH_2. With a larger bulk density, more propellant could be held in a given volume, so that, with no penalty in performance, a smaller vehicle could carry the same amount of propellant and consequently deliver the same payload to the target orbit. In reality, both effects work against each other, resulting in the actual curve that was minimized around 6.5. This trend was nearly independent of the liftoff T/W, with the optimal ratio of LOX to LH_2 weight being around 6.5 for values of liftoff T/W between 1.15 and 1.35 (Fig. 9).

A similar trade was conducted to determine the sensitivity of empty weight to liftoff T/W. The results of this trade, assuming a total O/F ratio of 6.0, are presented in Fig. 10. Each point on the curve was determined using the same iterative process that was used in the O/F trade. The empty weight was minimized when the liftoff T/W was approximately 1.23. Changing the T/W from 1.35 (reference) to 1.23 resulted in a 2% decrease in empty weight. If GLOW was minimized instead of empty weight (also shown in Fig. 10), the optimal T/W was somewhat higher (between 1.30 and 1.35). The optimal T/W differed between the two curves because the increase in engine weight that would accompany a higher liftoff T/W was a much larger percentage of empty weight than GLOW. Therefore, the performance benefit from a higher T/W was overcome by the added engine weight sooner when empty weight was minimized.

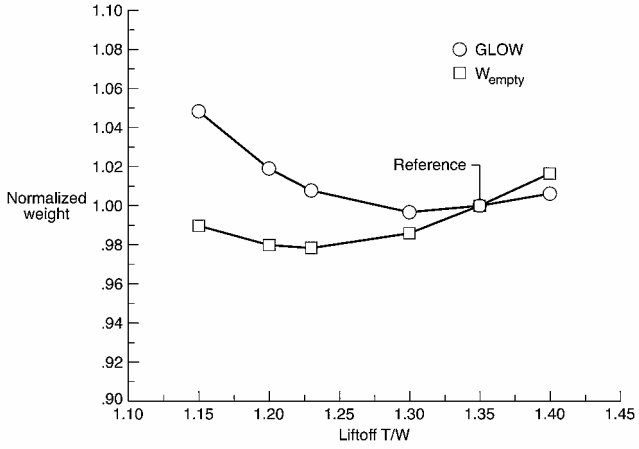

Fig. 10 Variation of GLOW and vehicle empty weight with liftoff *T/W* ratio (normalized with reference).

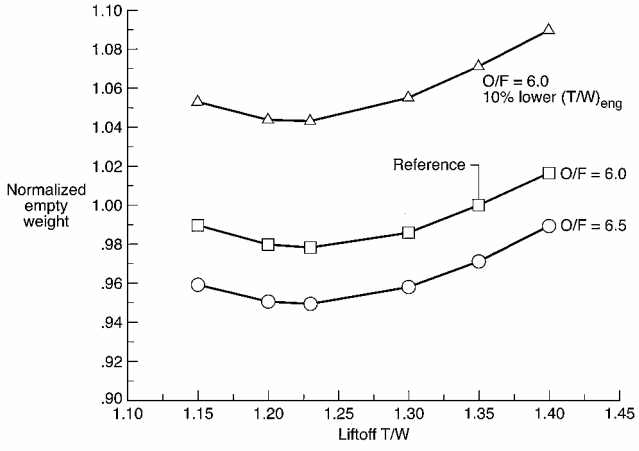

Fig. 11 Effect of *O/F* ratio and engine *T/W* on optimal liftoff *T/W* (normalized with reference).

Because cost is more closely related to the empty weight rather than GLOW, the lower T/W of 1.23 would likely lead to the lower cost configuration. However, the benefit in empty weight resulting from a lower T/W would have to be weighed against the effect such a change might have on the engine-out abort capability of the vehicle. With the linear aerospike engine considered in this study, a single engine-out is actually two engines-out. (An additional engine must be powered down to eliminate thrust imbalances between each side of the linear aerospike.) This would limit the lower T/W bound to about 1.25, assuming a 10% throttle-up of the remaining engines.

The trend of empty weight with liftoff T/W was independent of the total ratio of LOX to LH_2, with the optimal T/W being about 1.23 for O/F ratios between 6.0 and 6.5 (Fig. 11). As shown in Fig. 11, a 5% decrease in empty weight is possible by changing the reference values of liftoff T/W from 1.35 to 1.23 and total O/F from 6.0 to 6.5, abort concerns notwithstanding. Also in Fig. 11, the influence of the weight of the engine per pound of thrust (engine T/W) on the optimal value of liftoff T/W is shown. The engine T/W is a key input to the weights model and directly influences the weight of a number of propulsion system elements. For a decrease in engine T/W of 10%, the trend of empty weight with respect to liftoff T/W was unchanged, although the empty weight increased uniformly by over 6%.

Entry Trajectory Performance

An aerospace vehicle that operates in the hypersonic flight regime must be protected from the aerodynamic heating environment. The use of a relatively low-temperature (~1800°F maximum) metallic TPS has been proposed to meet this need for the lifting body configurations with large planform areas. In contrast, the current Space Shuttle Orbiter employs relatively high-temperature ceramic tiles (~2600°F maximum). Although the metallic system may offer some benefit in reduced maintenance requirements, its lower temperature capability necessarily constrains the vehicle flight envelope so that excessive heating levels are avoided. The lowest achievable peak laminar heating rate is a function of the vehicle configuration, hypersonic aerodynamics, and weight ($W/C_L S$) (Ref. 13). Based on the preliminary assessment shown in Fig. 12, it appeared possible, in theory, to maintain the laminar heating levels on the vehicle to within the limits required for the metallic TPS. However, turbulent heating levels can easily double the laminar values. Reference 14 illustrates the dramatic impact transition can have on TPS requirements, particularly in the case of a metallic system.

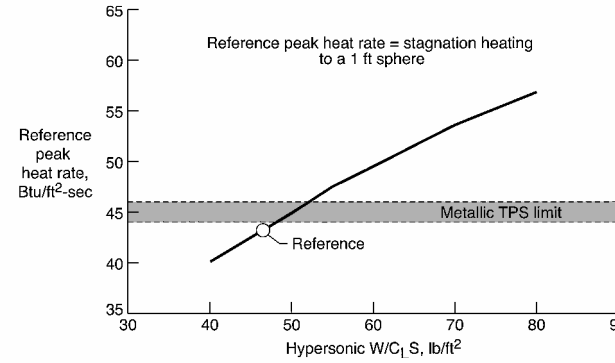

Fig. 12 Variation of peak reference heating rate with $W/C_L \cdot S$.

The objective of the entry trajectory development was to limit the laminar heating to levels within the capability of the proposed TPS and to delay the onset of transition such that turbulent heating levels did not exceed those experienced in the earlier laminar phase of the entry. A coupled approach that used POST and MINIVER together was employed to achieve these heating objectives and to satisfy other flight constraints such as the minimum crossrange requirement (750 n mile). Initially, a two-phased approach was used to develop an entry trajectory that met the thermal constraints. In the first phase, aerothermal constraints were imposed on the entry through the use of a reference heating indicator based on the work of Chapman.[15] This correlation, as applied in POST, is roughly proportional to $\rho^{1/2} V^3$. Although it is only an indicator of stagnation heating rates and loads, windward areas of the vehicle (where laminar continuum flow predominates) typically tend to track this indicator. Thus, it can be used directly in the optimization process if the appropriate target value can be determined. For this investigation, it was assumed that keeping the chine and nosecap regions below radiation equilibrium temperatures of 2000°F, was sufficient to limit most of the acreage to temperatures below the 1800°F allowable for the metallic TPS. Heat transfer distributions for the similarly shaped X-33 vehicle supported this assumption.[16] Transforming the temperature limit (2000°F) to a heating rate, adjusting for the vehicle scale, and applying a hot-wall correction resulted in the desired reference heating rate for the trajectory optimization process. This value (~45 Btu/ft^2-s) was very close to the theoretical minimum noted in Fig. 12.

Once a trajectory that met the laminar heating constraint was computed, the trajectory was postprocessed using MINIVER to determine the occurrence of transition and the expected laminar and turbulent heating levels at the vehicle surface. The thermal model used in MINIVER was the same as that used in Ref. 11, which was shown to yield excellent agreement with detailed computational fluid dynamics (CFD) predictions obtained for a similar lifting body configuration. The parameter used to predict transition onset in this study, Re_θ / M_e, is one that has been extensively validated in the shuttle program.[17] Unlike a simple length-based Reynolds number, this local parameter takes into account angle-of-attack effects, known to have a strong influence on the occurrence of transition. The transition work of Thompson et al.[18] led to selection of a value of 250 for this study. In the Thompson et al. paper, this parameter was predicted using the inviscid/boundary-layer code LATCH[19] and compared to experimental observations of transition on the X-33 forebody. A value of 300 was found to predict smooth-body transition results

accurately. Potential roughness elements on the metallic TPS led to the selection of the more conservative value of 250 for the work presented here.

An evaluation of the initial entry trajectory that was postprocessed using MINIVER indicated acceptable laminar but excessive turbulent heating rates. The high turbulent heating rates occurred because the optimized trajectory required flight at altitudes low enough to induce transition between 10,000 and 15,000 ft/s, where laminar heating rates were still fairly high. The flight profile was optimized at these lower altitudes because the density was higher and more lift could be generated to help meet the 750-n mile minimum crossrange requirement. This two-phase approach, in which a trajectory was first developed based on laminar heating constraints and then postprocessed to evaluate for transitional heating levels, was found to be cumbersome and failed to take advantage of the optimization capability within POST. An alternative approach was taken that indirectly coupled POST and MINIVER so that the transition parameter Re_θ/M_e could be used to influence the trajectory design. A series of MINIVER solutions were generated at a reference point immediately ahead of the expansion on the windward surface (90% of the vehicle length) for a range of velocities from 5000 to 17,000 ft/s and angles of attack from 20 to 50 deg. For each angle of attack and velocity, the altitude at which the transition parameter (Re_θ/M_e) reached a preselected value was determined. Tables representing a series of transition surfaces similar to the one shown in Fig. 13 were generated for transition parameter values ranging from 200 to 350. These tables were used to place additional constraints on the trajectory optimization to delay transition to as low a Mach number as possible.

The success of this approach depended on the ability of MINIVER to predict the transition parameter Re_θ/M_e accurately. This capability is demonstrated in Fig. 14 where MINIVER-based predictions were compared to predictions made using LATCH. This comparison is illustrative of the level of agreement between MINIVER and LATCH windward centerline predictions for the geometry of the study vehicle and the subscale X-33 demonstrator. Similar agreement was obtained for five other representative flight conditions ranging from Mach 10 to 20 and five angles of attack from 25 to 45 deg.

By the use of the existing reference heating calculation, together with the new transition tables, an optimized entry trajectory that targeted the desired heating rates and loads while simultaneously delaying the onset of transition to turbulent flow was generated. This optimized entry trajectory is presented in Fig. 15. The trajectory began with a deorbit maneuver from the ISS orbit that put the vehicle at atmospheric interface (altitude of 400,000 ft) with a flight-path angle of −1.1 deg. At this point, the angle-of-attack and bank angle profiles were tailored to minimize the reference heating rate and to meet the 750-n mile minimum crossrange requirement. In addition, the effect of trimming the vehicle in pitch using body flap and elevon deflections was modeled, and constraints were placed on the trajectory to ensure that the control surface deflections required for trim remained below 20 deg. Also, for this trajectory, transition was delayed to approximately Mach 9.3. To delay transition for as long as possible, the vehicle flew near the transition surface (Fig. 13) beginning at a velocity of approximately 12,000 ft/s until transition finally occurred near 10,000 ft/s. Subsequent heating predictions, based both on MINIVER and more detailed solutions using LATCH, indicated that peak laminar and turbulent heating levels were indeed within the capability of the metallic TPS. Figure 16 shows the effect of the crossrange requirement on the minimum peak heating rate for a typical lifting body configuration. As shown, lowering the 750-n mile requirement would not enable significantly lower peak heating rates.

The transition surfaces generated for this study cannot be applied directly to other configurations. However, the procedure to develop similar transition surfaces is straightforward. MINIVER has been successfully used to predict the windward centerline heating

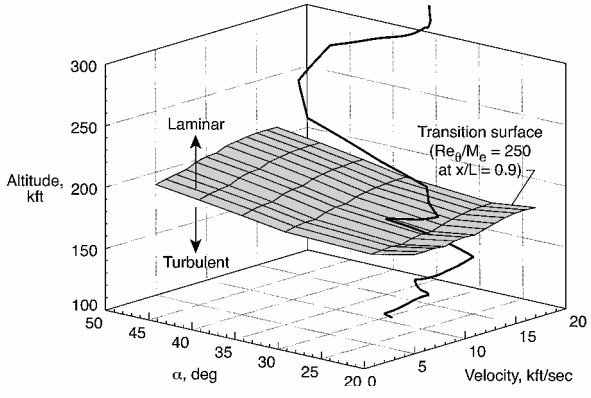

Fig. 13 Optimized entry trajectory and transition constraint surfaces.

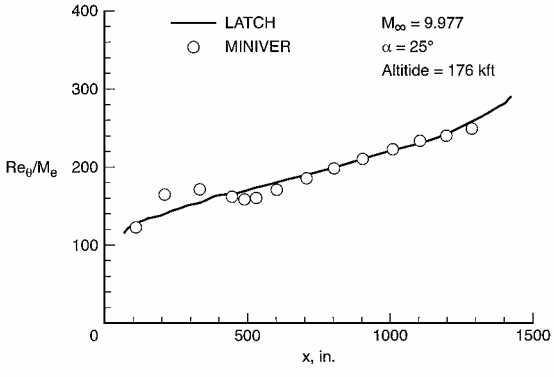

Fig. 14 MINIVER/LATCH Re_θ/M_e centerline comparison.

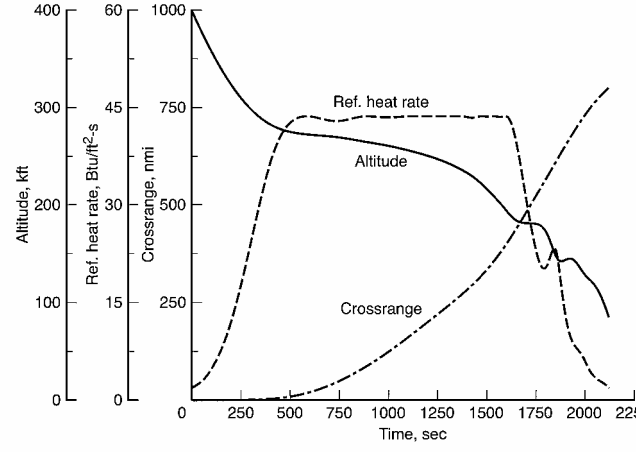

Fig. 15 Altitude, reference heating rate, and crossrange profiles for optimized nominal entry trajectory.

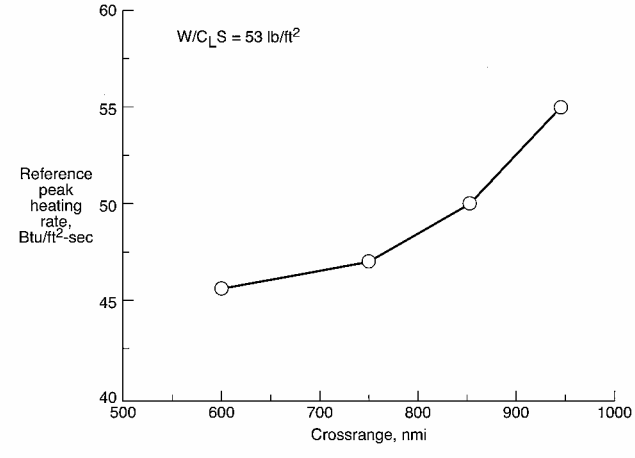

Fig. 16 Effect of minimum crossrange requirement on reference peak heating rate.

environments for a wide variety of configurations. When it is assumed that a reasonable assumption can be made for the transition value of Re_θ/M_e, surfaces similar to those developed here can be generated rapidly to aid in the trajectory development process for other vehicles. The integration of the aerothermal/TPS considerations directly within the trajectory optimization as developed here can potentially reduce the number of design cycles required to achieve the optimal trajectory/TPS balance for hypersonic flight vehicles.

Conclusions

As part of the X-33 program, conceptual studies were conducted that focused on the design, analysis, and screening of a range of full-scale SSTO configurations. These configurations integrated a linear aerospike engine into a lifting body configuration and employed a metallic TPS. This investigation presents the results of various performance trade studies that were performed in support of this effort. These trade studies were conducted using a multidisciplinary performance analysis approach that indirectly coupled trajectory optimization, weight estimation, and heating analysis tools.

The sensitivity of vehicle performance to a number of ascent trajectory constraints was determined. Results were presented that quantified the benefit of flying a lifting trajectory. Although the flight profile had to be limited so that structural design limits were not exceeded, using lift during ascent still resulted in an additional payload capability of over 1500 lb. In addition, it was found that the axial acceleration limit did not have a significant effect on payload capability, although altering it may ease engine-operating requirements. Finally, requiring the vehicle to be trimmed in pitch during ascent limited the range of angles of attack that could be flown and resulted in a payload penalty of roughly 1100 lb when compared to an untrimmed reference case where this requirement was ignored. Also, the pitch trim control authority of the linear aerospike thrust vector control system was relatively independent of longitudinal c.g. location. This insensitivity to c.g. location may be advantageous for a configuration with the LOX tank located in the aft end of the vehicle.

The linear aerospike engine had the ability to vary the mixture ratio during flight. Varying the mixture ratio in a steplike or continuous manner throughout the ascent increased the vehicle payload capability by nearly 2000 lb compared to the case in which it was held constant. Also, by variation of the mixture ratio profile, the total oxidizer-to-fuel ratio of the vehicle could be affected. Because this ratio influenced the weight and performance of the vehicle, its true effect could only be determined through an approach that coupled the vehicle sizing with the trajectory optimization. This approach was also used to determine the optimal liftoff thrust-to-weight ratio, which was directly related to the size of the engine. By changing the oxidizer-to-fuel ratio to 6.5 and the liftoff thrust-to-weight ratio to 1.23, the vehicle empty weight could be reduced by 5% compared to the reference case.

In addition to the ascent trajectory trades, coupled trajectory/thermal analyses were conducted to optimize the entry flight profile to the typical requirements of a metallic TPS. The objective of these analyses was to limit the laminar heating to levels within the capability of the proposed TPS and to delay the onset of transition such that turbulent heating levels did not exceed those experienced in the earlier laminar phase of the entry. Using an aerothermal analysis tool, transition surfaces were generated that could be used to predict transition onset as a function of altitude, velocity, and angle of attack. These surfaces were used directly by the trajectory optimization tool to achieve the heating objectives while meeting the minimum crossrange requirement of 750 n mile. Reducing the crossrange requirement did not result in significantly lower peak heating rates.

This study provided a broad view of a number of issues and concerns that should be considered in the performance analysis of a lifting body SSTO RLV. Emphasis was placed on the multidisciplinary nature of the analyses that were performed. It was necessary to couple the trajectory optimization with other discipline tools because changes in vehicle performance often affected the weight and design of many different systems. Capturing the effect of various design changes on both weight and performance is vital if the physical difficulty and small margins that characterize the design of a fully reusable single-stage launch vehicle are to be overcome.

Acknowledgments

The authors would like to thank Lockheed Martin Skunk Works for the opportunity to work with them on VentureStar and for the various data models that were provided by them during the course of this analysis. In addition, the authors would like to thank Anne Costa, who was instrumental in the preparation of this paper for publication.

References

[1]Stanley, D. O., Engelund, W. C., Lepsch, R. A., McMillin, M., Wurster, K. E., Powell, R. W., Giunta, T., and Unal, R., "Rocket-Powered Single-Stage Vehicle Configuration Selection and Design," *Journal of Spacecraft and Rockets*, Vol. 31, No. 5, 1994, pp. 792–798.

[2]Stanley, D. O., Engelund, W. C., and Lepsch, R. A., "Propulsion System Requirements for Reusable Single-Stage-to-Orbit Rocket Vehicles," *Journal of Spacecraft and Rockets*, Vol. 31, No. 3, 1994, pp. 414–420.

[3]Freeman, D. C., Jr., Talay, T. A., Stanley, D. O., Lepsch, R. A., and Wilhite, A. W., "Design Options for Advanced Manned Launch Systems," *Journal of Spacecraft and Rockets*, Vol. 32, No. 2, 1995, pp. 241–249.

[4]Baumgartner, R. I., and Elvin, J. D., "Lifting Body: An Innovative Reusable Launch Vehicle Concept," AIAA Paper 95-3531, Sept. 1995.

[5]Lockwood, M. K., "Overview of Conceptual Design of Early VentureStar Configurations," AIAA Paper 2000-1042, Jan. 2000.

[6]Brauer, G. L., Cornick, D. E., and Stevenson, T., "Capabilities and Applications of the Program to Optimize Simulated Trajectories (POST)," NASA CR-2770, Feb. 1977.

[7]Lepsch, R. A., Stanley, D. O., and Unal, R., "Dual-Fuel Propulsion in Single-Stage Advanced Manned Launch System Vehicle," *Journal of Spacecraft and Rockets*, Vol. 32, No. 3, 1995, pp. 417–425.

[8]Korte, J., "Parametric Model of an Aerospike Rocket Engine," AIAA Paper 2000-1044, Jan. 2000.

[9]Engel, C. D., and Praharaj, S. C., "MINIVER Upgrade for the AVID System, Vol. I: LANMIN User's Manual," NASA CR-172212, Aug. 1983.

[10]Wurster, K. E., Riley, C. J., and Zoby, E. V., "Engineering Aerothermal Analysis for X-34 Thermal Protection System Design," *Journal of Spacecraft and Rockets*, Vol. 36, No. 2, 1999, pp. 216–228.

[11]Gnoffo, P. A., Weilmuenster, K. J., Hamilton, H. H., Olynick, D. R., and Venkatapathy, E., "Computational Aerothermodynamic Design Issues for Hypersonic Vehicles," *Journal of Spacecraft and Rockets*, Vol. 36, No. 1, 1999, pp. 21–43.

[12]Wurster, K. E., and Stone, H. W., "Aerodynamic Heating Environment Definition/Thermal Protection System Selection for the HL-20," *Journal of Spacecraft and Rockets*, Vol. 30, No. 5, 1993, pp. 549–557.

[13]Wurster, K. E., and Eldred, C. H., "Technology and Operational Considerations for Low-Heat-Rate Trajectories," *Journal of Spacecraft and Rockets*, Vol. 17, No. 5, 1980, pp. 459–464.

[14]Wurster, K. E., "Assessment of the Impact of Transition on Advanced Winged Entry Vehicle Thermal Protection System Mass," AIAA Paper 81-1090, June 1981.

[15]Chapman, D. R., "An Approximate Analytical Method for Studying Entry into Planetary Atmospheres," NACA TN-4276, May 1958.

[16]Hamilton, H. H., II, Weilmuenster, K. J., Horvath, T. J., and Berry, S. A., "Computational/Experimental Aeroheating Predictions for X-33 Phase 2 Vehicle," AIAA Paper 98-0869, Jan. 1998.

[17]Bouslog, S. A., An, M. Y., and Derry, S. M., "Orbiter Windward-Surface Boundary-Layer Transition Flight Data," NASA CP-3248, April 1995.

[18]Thompson, R. A., Hamilton, H. H., II, Berry, S. A., Horvath, T. J., and Nowak, R. J., "Hypersonic Boundary-Layer Transition for X-33 Phase 2 Vehicle," NASA TM-1998-207316, Jan. 1998.

[19]Hamilton, H. H., II, Greene, F. A., and DeJarnette, F. R., "Approximate Method for Calculating Heating Rates on Three-Dimensional Vehicles," *Journal of Spacecraft and Rockets*, Vol. 31, No. 3, 1994, pp. 345–354.

J. A. Martin
Associate Editor